

# The generation of nondiffracting beams using inexpensive computer-generated holograms

Carlos López-Mariscal and Julio C. Gutiérrez-Vega

*Photonics and Mathematical Optics Group, Tecnológico de Monterrey, Monterrey, Mexico 64849*

(Received 3 March 2006; accepted 8 September 2006)

We present a simple experimental procedure for producing a computer-generated hologram of good quality. As an example, the transverse intensity and phase structure of nondiffracting beams is investigated. © 2007 American Association of Physics Teachers.

[DOI: 10.1119/1.2359001]

## I. INTRODUCTION

Because laser applications are found in a wide variety of scientific and engineering disciplines,<sup>1</sup> the dynamics of wavefields associated with laser beams are of special interest in the undergraduate physics curricula. One problem arises when a laser beam is to be shaped to a particular profile. For most applications, it is desirable that most of the laser energy be confined to a small spot. Many laser resonators readily yield a beam with this characteristic, namely a Gaussian beam. The spot size of a laser beam is affected by diffraction as the beam propagates, which results in a limited useful range of propagation. The more tightly a laser beam is focused, the faster it will diverge. Diffractive spreading limits the useful range of lasers in areas such as metrology, free-space communications, and optical lithography.<sup>2</sup>

Alternate beam shapes are more convenient for certain applications. For instance, in laser surgery for vision correction, an annular beam is sometimes required to ablate annular sections of tissue from the cornea. Application-specific beam shaping can be achieved in several ways. For instance, when a Gaussian beam is incident on a specifically tailored hologram, the shape of the beam is modified according to the information encoded in the hologram. This phenomenon can be exploited to generate a beam with an arbitrary profile. In this paper we present a simple step-by-step technique for this purpose.

Recipes for making holograms have been the subject of several popular articles (see, for instance, Ref. 3). Many papers explaining the operating principles of holography at the undergraduate level are available, some of which stress the experimental techniques and their implementation. In particular, Ref. 4 is a useful starting point for the newcomer to holography. It pinpoints many practical aspects to be taken into consideration for the successful generation of holograms. There are also several articles<sup>5-8</sup> that describe detailed procedures to make computer-generated holograms. For example, Marsh and Smith<sup>5</sup> took advantage of an early programmable calculator with graphical capabilities to compute and plot Fourier computer-generated holograms of simple objects. This technique can now be used with desktop computers to make holograms of objects of much greater complexity. Similarly, Chen and colleagues<sup>6</sup> took a picture of a computer-generated hologram in a computer display with only a few samples and used their negatives as downscaled holograms with very good results. Leming and Hastings<sup>7</sup> devised a particularly ingenious experiment that demonstrates how the calculation of a hologram is done and how the hologram is constructed. In their procedures for the microwave regime, they utilize aluminum foil and construction paper

with holographic techniques that are the analog of those used with visible light. More recently, Seymour<sup>8</sup> documented a simple recipe for the generation of computer-generated holograms using a personal computer of the kind available 10 years ago.

The purpose of this paper is to show how undergraduate students can produce good quality, low cost computer-generated holograms for the purpose of shaping a beam to a particular profile. We sketch a simple procedure to calculate holograms using a computer, and we explain how to record them using photographic film. It is assumed that the student has programming skills and is knowledgeable about basic photographic and dark room techniques. This paper is self-contained and students are encouraged to regard the results as a starting point to explore the physical principles of digital holography. We also hope to serve the undergraduate laboratory instructor seeking a lab exercise to demonstrate holographic methods.

We have purposely chosen to use computer-generated holograms to generate Bessel beams. Their study introduces the principles of propagation for this class of beams, which constitute an alternative to Gaussian beams and their limiting Rayleigh range, and thus provides possible applications in many fields of technology.<sup>9</sup>

## II. REVIEW OF FUNDAMENTAL CONCEPTS

We give a brief review of the fundamental concepts of nondiffracting beams and digital holography. The reader with previous experience in these fields may want to proceed directly to Sec. III.

### A. Nondiffracting beams

There exists a particular kind of nondiffracting laser beam that, in contrast to a Gaussian beam, can propagate while its transverse shape remains unaltered. In other words, a slice of the beam remains unchanged and does not suffer from the natural diffractive spreading to which all other wavefields are subject. This property is a consequence of the way in which the beam depends on the spatial coordinates. More specifically, nondiffracting wavefields are spatially described by the product of two functions. One of the functions describes the transverse field, or the shape of a “slice” of the beam perpendicular to the propagation axis. The other function describes the way in which the field varies as it travels in the propagation direction, say,  $z$ . Both functions are in general complex. For nondiffracting beams the transverse field is independent of  $z$ . The longitudinal field depends only on  $z$ , and it does so such that only the phase of the wavefield varies

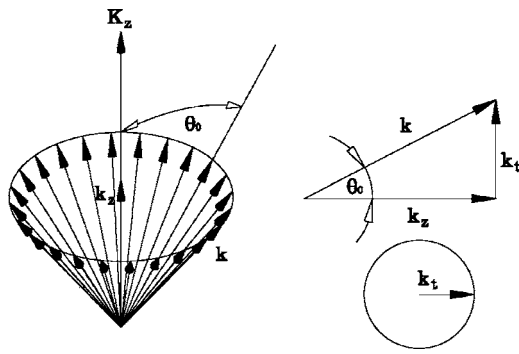


Fig. 1. Wavevectors that describe a nondiffracting wavefield. All plane waves in the wavefield have the same inclination  $\theta_0$  with respect to the propagation axis.

with  $z$ , but not the amplitude. Hence, as the beam propagates, there is no perceptible change in its transverse intensity because this intensity is proportional to the square of the amplitude of the field. More details on nondiffracting beams can be found in Refs. 10 and 11.

The propagation of a wavefield in general is governed by a solution to the Helmholtz equation. A nondiffracting solution can be found when the equation is separable, that is, when it can be expressed as the product of a transverse and a longitudinal field. Separability of the Helmholtz equation occurs only in four coordinate systems. Accordingly, there are four fundamental classes of nondiffracting beams. Depending on the symmetry imposed by the coordinate system, the transverse solution is characterized by at least one parameter, which is termed the order of the solution.

In practice, the electromagnetic fields associated with nondiffracting beams require an infinite amount of energy to propagate unaltered an arbitrarily long distance,<sup>12</sup> and thus they are not physically realizable. Nevertheless, it is possible to generate good approximations in the laboratory that will propagate in a similar way to their theoretical counterparts for a limited distance.

Nondiffracting beams are not only unaffected by diffractive spreading, but also are capable of self-reconstructing. In other words, when a small opaque object is placed in the path of a nondiffracting beam, the wavefield appears to reconstruct its initial profile after it propagates for a short distance.<sup>13</sup> This behavior makes them suitable for applications where the same beam activates two colinear optical gates, such as in the optical interconnect of two distant circuit boards.<sup>14</sup>

The characteristic feature of nondiffracting beams in Fourier space is that their angular spectrum lies on a thin annulus. This property means that if we were to obtain the optical Fourier transform of a nondiffracting beam, we would observe a thin, bright ring. In the laboratory, the optical Fourier transform of a transverse field is commonly obtained by means of a converging lens. The power spectrum can be observed in the focal plane of the lens and represents the spatial frequency content of the beam. As a consequence, it is said that the angular spectrum of a nondiffracting beam is made up of wavevectors that lie on the surface of a cone. This wavevector distribution is equivalent to thinking of a nondiffracting beam as a superposition of plane waves that have the same inclination  $\theta_0$  with respect to the propagation axis, as shown in Fig. 1. Here the wavevector  $k$  has the same

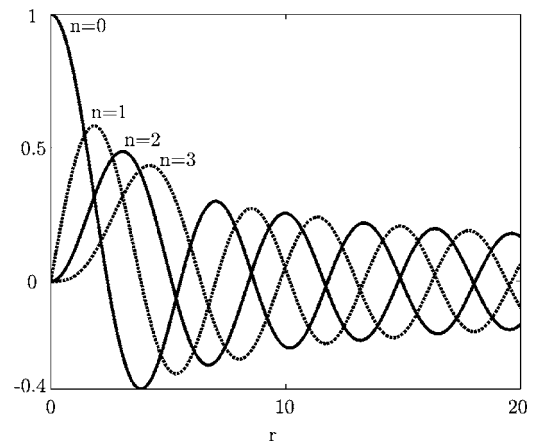


Fig. 2. Bessel functions of the first kind  $J_n(r)$  for  $n=0, 1, 2$ , and  $3$ .

magnitude for all plane waves, and  $k_t$  and  $k_z$  are its transverse and longitudinal components. In this case the transverse components of all the wavevectors follow the locus of a circle centered at the intersection of the propagation axis and the Fourier plane. Hence the shape of the angular spectrum is a thin ring.

Each class of nondiffracting beams is essentially different in the functional form of its transverse fields, and hence their angular spectrum will also be distinct. Although the spectrum still has the shape of a thin ring for all families, the intensity of the ring varies with the azimuthal angle, meaning that some of the plane waves that make up the spectrum have greater amplitude than others, yet their inclination with respect to the propagation axis is the same. Additionally, the relative phase of each of the constituting plane waves can also be varied, thus giving different fields that are nondiffracting. In other words, for a nondiffracting beam, the value of the field anywhere in the annular extent of its angular spectrum is in general complex and arbitrary.

In Cartesian coordinates the Helmholtz equation is satisfied by all plane waves with a constant inclination  $\theta_0$  with respect to the propagation axis  $z$ . The wavevectors of all the possible waves that satisfy this condition lie in the surface of a cone in frequency space as shown in Fig. 1. Each plane wave or combination of plane waves associated with these wave vectors is a valid solution. Note that a plane wave in this case is a mathematical entity that extends indefinitely in the spatial coordinates and its wavefronts of constant phase are described by infinite planes. Such plane waves would indeed be nondiffracting. In the laboratory this field can only be approximated in a limited spatial extent by a flat top beam or the interference of several of them.

The particular case of circular cylindrical coordinates has been extensively studied, especially for the lowest-order solution. Because this coordinate system is circularly symmetric, the same is expected of the solutions to the Helmholtz equation. The modes are given by Bessel functions of the first kind, and the order can be any positive integer and zero. A plot of the first four Bessel functions of the first kind is shown in Fig. 2. Note that the amplitude of the functions is larger near the origin and that the fundamental ( $n=0$ ) Bessel function has a maximum at the origin; for higher orders the value of the function vanishes there. Also note that the functions are oscillatory and the relative amplitude of the first maximum decreases with the order.

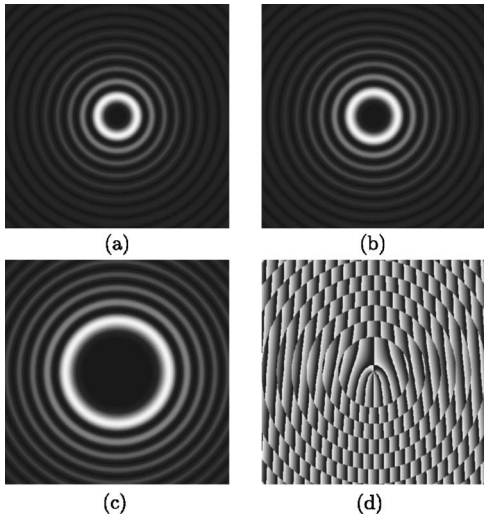


Fig. 3. Transverse intensity profiles for Bessel beams of order (a)  $m=4$ , (b)  $m=5$ , and (c)  $m=12$ . Also shown in (d) is the spatial phase distribution of interference of a Bessel beams of fourth order and an inclined plane wave in a plane perpendicular to the propagation axis.

Bessel beams are circularly symmetric, and thus all wavevectors of the cone in frequency space are included in their spectrum and have the same amplitude regardless of their angular position. These wavefields have a characteristic phase distribution. For  $n \neq 0$ , the transverse phase distribution varies linearly with respect to the azimuthal coordinate. The transverse field solution is thus described by

$$u_t(\mathbf{r}_t) = J_m(k_t \mathbf{r}_t) e^{im\varphi}, \quad (1)$$

where  $m=1, 2, 3, \dots$  is the order of the Bessel function. The best known example of a nondiffracting beam is the zeroth-order Bessel beam.<sup>15,16</sup> In this case the center of the beam is a bright spot, whereas for higher orders, the center is a field minimum, that is, a dark spot as expected from the Bessel functions (see Fig. 2).

A quantitative comparison of the spreading of the central spot of a zeroth-order Bessel beam and a Gaussian beam with a waist of the same size as the spot shows that the former propagates for a considerably longer distance than the latter before having a measurable spread.<sup>17</sup> The transverse intensity profiles associated with Bessel beams of different orders are plotted in Fig. 3. The total energy in every lobe of a Bessel beam is approximately the same.

Also plotted is the transverse phase distribution that results from the interference of a Bessel beam of fourth order with a plane wave inclined in the horizontal direction. Note that adjacent concentric lobes differ by a value of  $\pi$  in phase because, for a fixed angular position, the bright and dark fringes alternate radial positions.

The phase variation  $m\varphi$  of Bessel beams of order  $m > 0$  results in an additional interesting property, namely, its orbital angular momentum. In contrast to the spin angular momentum of the beam, orbital angular momentum arises solely because of the phase variation of the beam and it is not related to its state of polarization. Angular momentum carried by the beam can be effectively transferred to material particles, thus setting them into rotational motion.<sup>18</sup>

## B. Computer-generated phase holograms

A hologram is essentially a record of the interference of two coherent fields: a reference wavefield and a signal wavefield of the same wavelength that contains information on the object of interest.<sup>4</sup> For this reason, a hologram is sometimes referred to as an interferogram. A setup for making holograms usually involves the splitting of a laser beam to obtain the two required wavefields from the same source. Typically, the reference wavefield is a plane wave and the signal is provided by the light that has been reflected from the surface of the object. As in any interferometric experiment, care must be taken to ensure that the total optical path difference between both beams is not larger than the coherence length of the laser being used.

It is customary to use holographic plates as media to store the record of the interferogram. In essence holographic plates differ from photographic film only in that the former are capable of storing information at much higher spatial densities or resolution than the latter. A typical spatial resolution for photographic film is 90 lines per mm (lpm), whereas for plates this value ranges from 1000 to 5000 lpm. For comparison, a currently available laser printer has a typical resolution of about 5 lpm. Holographic plates are sometimes mounted on a glass substrate instead of the more common acetate backing. This backing gives plates the additional advantage of being less vulnerable to deformation from thermal effects or aging.

We can readily reproduce the wavefield from the interferogram recorded in the film or plate. To reconstruct the wavefront originally reflected from the object, we illuminate the hologram with a plane wave of the same inclination and wavelength as the reference used in the recording process. Because the plane wave has a constant phase wavefront, it will acquire the phase distribution stored in the plate, thereby creating a virtual image of the object.

Roughly speaking, there exist two kinds of holograms depending on whether the reconstruction of the registered object is made by transmission or reflection of light by the holographic plate. More complex holographic techniques include multiple exposure of test subjects under vibration or strain and storing of holographic data on optical media for computing applications.

Because making a hologram requires only the superposition of the object and reference wavefields, it is possible to calculate the interferogram by means of a computer. Such a process yields a computer-generated hologram. Clearly, the making of a computer-generated hologram does not require the object in which we are interested to exist, which is a significant advantage of computer-generated holograms over traditional holograms.

Computing the interferogram of a complex field involves adding the complex transverse field  $E(\mathbf{r}_t)$  and an inclined plane wave  $E_{\text{ref}}(\mathbf{r}_t)$ , where  $\mathbf{r}_t$  are the transverse coordinates. For instance,  $E_{\text{ref}}(\mathbf{r}_t) = E_0 \cos(k_t x)$ , where  $k_t = k \cos \gamma$ ,  $k = 2\pi/\lambda$  is the wavenumber, and  $\gamma$  is the relative angular displacement between the reference wavevector and the propagation axis of the object field. The relative phase difference of the object and reference fields will determine the local intensity of the interferogram. A maximum amplitude region results where the interference is constructive, that is, both interfering wavefields are in phase. When the relative phase of the interference field,  $E(\mathbf{r}_t) + E_0 \cos(k_t x)$ , is exactly a half-wave, a zero-valued amplitude of the local field results. A

range of amplitude values will result for the different relative phases of the object and reference wavefields.

In this way we can plot only the phase of the interferogram, discarding information about the amplitude, and hence obtain an approximate description of the interferogram, which is accurate regarding its phase but not its amplitude. More complex and ingenious schemes to preserve and encode both the amplitude and phase of the hologram have been devised,<sup>19–21</sup> but we have used this simple approach in our experiment. For some applications, it is customary to refer to  $E_{\text{ref}}(\mathbf{r}_t)$  as the carrier wave, because it is represented by a periodic spatial signal that is modulated with the phase information contained in  $E(\mathbf{r}_t)$  when computing the hologram. Following the sampling theorem, the spatial frequency of  $E_{\text{ref}}(\mathbf{r}_t)$  should be at least twice the highest spatial frequency of  $E(\mathbf{r}_t)$ , assumed here to be band limited. Because only a limited spatial extent of the field  $E(\mathbf{r}_t)$  is sampled, we would expect that its angular spectrum will be reconstructed up to some error.

If the values of the resulting interferogram are sampled and a grayscale value is associated with every sample, then the computer-generated hologram is termed a *blazed* hologram because of its appearance. In some cases it may be more convenient to limit the possible values of the samples to either 1 or 0, in which case a *binary* hologram is created. The amplitude resolution of the former is greater than that of the latter, which results in better fidelity for the *blazed* hologram.

### C. Blazed computer-generated holograms with photographic film

Registering the values of the calculated interferogram can be done in one of several ways. One option is to use a slide writer, which was originally used for the photoreduction of computer display output directly onto photographic film. A more accurate method is to use a laser or an electron beam to etch a glass substrate or lithographic film, which yields resolution values comparable to or higher than holographic plates. This procedure is called laser or electron beam (e-beam) lithography. In e-beam lithographic methods, the interferogram is recorded as thickness variations in the glass substrate. These result in a change of the local optical path length, which causes a delay in the phase of the reconstruction wavefield, thus shaping it by modifying the phase distribution of the incident wavefront. For this reason, such computer-generated holograms are termed phase holograms. In laser lithography a diffraction-limited laser spot is used to write directly onto the lithographic film with very high contrast. Alternatively, when using a holographic plate, the interferogram is recorded as a fringe pattern in the emulsion with varying optical densities, which is then referred to as an amplitude hologram. Note that an amplitude hologram obscures sections of the incident wavefront, whereas the phase hologram only modifies its phase. Hence, the former is less efficient than the latter. An amplitude hologram stored in photographic film or a holographic plate can be converted into a phase hologram by a chemical process known as bleaching.<sup>22</sup> This process procures the rehalogenation of the metallic silver grains in the developed emulsion and turns the stored hologram transparent, while preserving the thickness variations of the emulsion on the plate.

Despite its low resolution, commercial photographic black

and white film can be used to store computer-generated holograms with reasonably good accuracy for our purposes. In our experiment we created the interferograms of complex transverse field profiles using a computer program. We then showed the interferograms on a computer display and transferred the interferogram to photographic negative film using an ordinary single-lens reflex camera. The hologram can then be bleached, but this step is optional and requires chemical solutions not always available in the undergraduate laboratory. One advantage of photographic film over holographic plates is that its developing process is simple and inexpensive, whereas some plates require more intricate processes and specialized chemicals.

### III. EXPERIMENTAL SETUP

An experiment that is simple to reproduce and serves the purpose of observing nondiffracting beams is described in this section. Undergraduate students can reproduce our results with relatively little effort and can do further experiments by modifying the basic setup to make additional measurements.

The computer-generated holograms of the desired field distributions can be calculated. This calculation is straightforward because the transverse field distribution of the fields is known. In our case, we used MATLAB,<sup>24</sup> but an equivalent routine in C/C++ or any other programming language can be implemented. The algorithm can be summarized as follows:

- (1) Calculate  $E(\mathbf{r}_t) + E_{\text{ref}}(\mathbf{r}_t)$ . For instance:  $J_m(k_t \rho) e^{im\varphi} + \cos(nk_t \rho \cos \varphi)$ , where  $n > 1$  is a measure of the degree of inclination of  $E_{\text{ref}}(\mathbf{r}_t)$  relative to  $E(\mathbf{r}_t)$ .
- (2) Compute the argument of  $E(\mathbf{r}_t) + E_{\text{ref}}(\mathbf{r}_t)$  and obtain its value modulo  $2\pi$ .
- (3) Normalize the result to values between 0 and 1.

The result of this operation is a numerical value between 0 and 1 for every point in the spatial extent determined by  $\rho$  and  $\theta$ . This value represents the amplitude of the interference of  $E(\mathbf{r}_t)$  and the inclined reference wavefront  $\cos(nk_t \rho \cos \varphi)$ , because the argument represents the relative phase of their superposition and thus the resulting magnitude up to a constant factor.

The interferograms are now ready to be rendered as grayscale plots in a computer display. Note that the phase term added by  $E_{\text{ref}}(\mathbf{r}_t)$  is a sawtooth function that varies linearly between 0 and  $2\pi$ , thus acting as a diffraction grating. Taking a photograph of the display under no illumination other than the display itself will serve the purpose of recording the hologram in the film while reducing the hologram in size. Note that negative film will actually acquire a grayscale pattern that is the complement of the image in the display. This difference is not relevant for the experiment because it is equivalent to an overall phase factor of the interferogram.

For Bessel beams the holograms will resemble the annular structure of the beams, as shown in Fig. 4. It is easy to see from these plots that the structure of the higher-order Bessel beam is different from the zeroth order. If we keep in mind that gray levels are related to the phase of the field in a particular point, it is natural that the central pattern in Fig. 4(b) is referred to as a phase singularity. This particular feature is closely related to the orbital angular momentum of the beam.

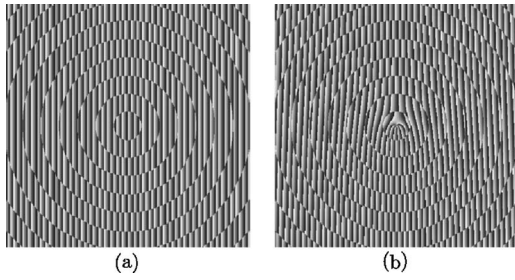


Fig. 4. Computer-generated holograms of Bessel beams of order (a)  $m=0$  and (b)  $m=5$ ,  $1024 \times 1024$  pixels. After photoreduction, they are  $4.5 \times 4.5$  mm in the film.

We used ILFORD PAN F Plus ASA 50 negative film and a Canon SLR camera (AE-1) with a standard 50 mm objective lens. Photographs taken from a distance of 3.5 m away from a carefully aligned 17 in. display worked well. While photographing the display, it is advisable to bracket the exposure times and the aperture in half steps to compensate for a possible low light reading of the exposure meter. We found that a combination of  $f\# = 8$  and exposure time of 0.25 s yields the best results for our monitor and film. These figures can be used as a first approximation in replicating the experiment and may vary depending on the intensity of the display, the sensitivity of the film, and the aperture of the camera.

The film can be developed in the usual way. We used Kodak HC-110 developer (dilution B), Kodak indicator stop bath, and Kodak rapid fixer following the recommended times and concentrations; other equivalent products should yield similar results. The holograms that work best are those with a wide range of gray levels when inspected with a loupe. Very light (underexposed) holograms proved ineffective at diffracting light; very dark negatives absorb a large proportion of the incident reference beam and the intensity after the hologram is low.

The hologram is backlit with a collimated plane wave, for instance, from a low-power He-Ne laser. We used a spatial filter made of the combination of a  $10\times$  microscope objective and a  $25 \mu\text{m}$  pinhole and a collimating lens for plane wave illumination of the hologram. A positive lens with focal length  $f_1$  placed one focal length in front of the hologram will allow for the angular spectrum to be observed one focal length ahead of the lens (see Fig. 5). In each of the  $\pm 1$  dif-

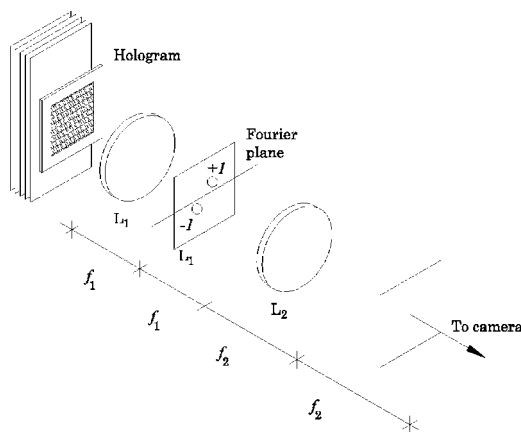


Fig. 5. Experimental setup for the reconstruction of the computer-generated hologram. The hologram is retro-illuminated with a plane wavefront.

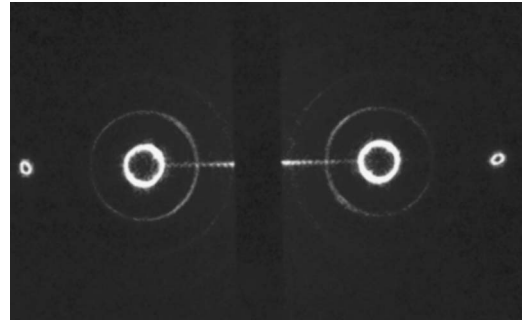


Fig. 6. Photograph of the transverse intensity at the Fourier plane. Note the two bright rings that correspond to the  $+1$  and  $-1$  diffraction orders. The smaller rings toward the edges of the photograph correspond to the  $-2$  and  $+2$  diffraction orders. The zeroth order has been purposely obstructed.

fraction orders at least one thin, bright ring should be clearly visible. These rings are specular images of each other about the propagation axis, as shown in Fig. 6. Their position depends on the inclination given to the plane wave used to construct the hologram. The more inclined the plane wave is with respect to the propagation axis, the further away from the axis is the location of the first diffraction order. This displacement is evident if we think of the carrier as a diffraction grating, where the pitch of the grating is inversely proportional to the spacing of the diffraction orders.

Because the backing of photographic film is far from perfect, and so is the granular structure of its emulsion, the images will be somewhat noisy due mainly to scattered light. Additionally, the zeroth diffraction order is an important source of unwanted noise. To use the spectrum as the annular source for a nondiffracting beam, it is necessary to filter out all the light not associated with one of the annuli, for instance, the one in the  $+1$  diffraction order, although the  $-1$  order counterpart could be used just as well. We can block all the unwanted light using a circular diaphragm (not shown) as a pupil. It is important that the diffraction orders in the Fourier plane be sufficiently separated from the zeroth order of diffraction so as to be able to isolate one ring. Once the annulus is filtered, a second lens  $L_2$  with focal length  $f_2$  should be placed one focal length ahead of the Fourier plane as shown in Fig. 5. This second lens produces the Fourier transform of the spectrum, thus generating the desired beam. The focal length of the lenses should be chosen so that the annulus is slightly larger than the smallest aperture to which the diaphragm can be set. In our case  $f_1 = 15$  cm and  $f_2 = 35$  cm.

We used a Fourier hologram to generate the angular spectrum of the beam. This method is equivalent to using a backlit thin annular slit, because an annular source acts like the angular spectrum and is then Fourier transformed by a lens. By using a hologram, we can generate an arbitrary nondiffracting beam by including the amplitude and phase modulation of the ring; for an annular slit only a zeroth-order Bessel beam can be generated. In both cases the purpose is to devise a ring composed of point sources of spherical waves to a good approximation. Because the spherical waves originate in the back focal plane of lens  $L_2$ , they are all collimated after the lens and thus form the plane wave superposition that shape the desired nondiffracting beam.

If desired, a photographic camera can be placed in front of lens  $L_2$ . The plane located a distance  $f_2$  ahead of lens  $L_2$  is

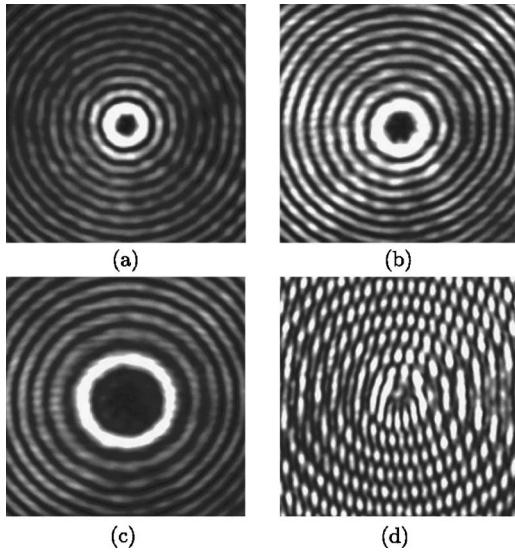


Fig. 7. Photograph of the transverse intensity profiles of Bessel beams of order  $m$  for (a)  $m=4$ , (b)  $m=5$ , and (c)  $m=12$ . Interference of the Bessel beam of order 4 and an inclined plane wave is shown in (d).

conjugate to the plane of the hologram, and the evolution of the transverse intensity profile can be investigated after propagation from this point on. Displacing the camera along the propagation axis and photographing the transverse intensity profile at several distances will show how the transverse intensity behaves as the beam propagates. We used our SLR camera for this purpose, first removing the objective lens and aligning the beam with the center of the camera aperture. Care should be taken at this point not to look into the camera eyepiece.

We can also use a lensless digital camera for this purpose if a neutral density filter is used to avoid saturation or damage to the camera due to the high intensity of the laser. Photographic paper can also be used, in which case the recording of the intensity patterns must be done in complete darkness.<sup>23</sup>

#### IV. OBSERVATION OF NONDIFFRACTING BEAMS PARAMETERS

##### A. Transverse intensity and propagation

Bessel beams can be observed by setting  $E(r_t)$  as given in Eq. (1). For instance, the transverse intensity profiles for  $m=0, 1, 4$ , and  $15$  are shown in Fig. 7. The characteristic concentric lobes should be clearly defined and the innermost lobe should be considerably more intense than the surrounding ones. We can also observe features that differ from one order to another. For example, the circular shadow in the center of high-order Bessel beams becomes more extended as the order increases, while the spacing of the outer lobes remains nearly constant.

More interesting than observing the transverse intensity profile alone is its comparison at different distances from the second lens. Contrary to what might be expected for a Gaussian beam, there should be essentially no change in the size or shape of the intensity pattern. For example, the profile of the fourth-order Bessel beam was recorded one focal length ahead of lens  $L_2$  and 1 m further ahead along the propagation axis; the photographic record of the intensity at

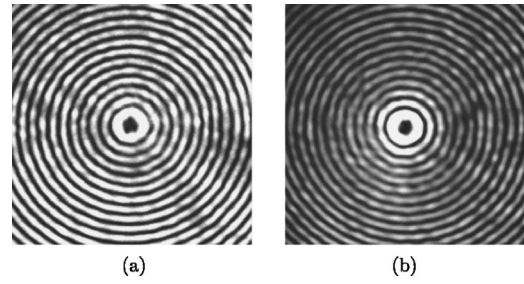


Fig. 8. Photograph of the transverse intensity profile of the Bessel beam of fourth order at (a)  $z_1=f_2$  and (b)  $z_2=z_1+1$  m. The mean diameter of the central lobe is  $750 \mu\text{m}$ .

the two different planes is shown in Fig. 8. All nondiffracting beams are expected to behave in the same way regardless of their order. As long as the value of  $k_t$  remains the same, the beam will be nondiffracting for the same distance.

It is also evident that the outer lobes in Fig. 8(b) are less intense than in Fig. 8(a). This intensity distribution is consistent with the fact that the central region of the beam will propagate unchanged for the longest distance  $z_{\text{max}}$ , because the plane waves that form the Bessel beam interfere at the optical axis for a longer distance than they do far away from it (see Fig. 9). Interference results in a conical region of invariance of length  $z_{\text{max}}$ , which can be estimated geometrically from the angular magnification of one point in the angular spectrum as  $z_{\text{max}}=R_2 f_2/a$ , where  $R_2$  is the radius of lens  $L_2$  and  $a$  is the radius of the ring in the Fourier plane. In our experiments,  $R_2$  is 4.5 cm and  $a$  is 0.5 mm, which yields  $z_{\text{max}}=31.5$  m. The central lobe of the beam is  $535 \mu\text{m}$  in radius, in comparison to the Rayleigh range of roughly 1.5 m for a Gaussian beam with waist  $\omega_0=535 \mu\text{m}$ .

One additional experiment can be undertaken once the beam has been successfully observed. To investigate the phase distribution of our beam, the interference pattern that results when the first-order Bessel beam interferes with a plane wave was recorded in Fig. 7(d). The fringe pattern appears to have vertical periodicity because the phase of the inclined wave varies with the horizontal axis. In other words, the plane wave is inclined in the horizontal direction with respect to the propagation axis of the nondiffracting beam.

For comparison, note that Fig. 3(d) is characterized by having a richer grayscale range of values; however, Fig. 3(d) represents a phase distribution whereas Fig. 7(d) is a photograph of intensity levels that result from the interference of a Bessel beam with its characteristic phase variation and a plane wave. From the fringe pattern in this photograph, we

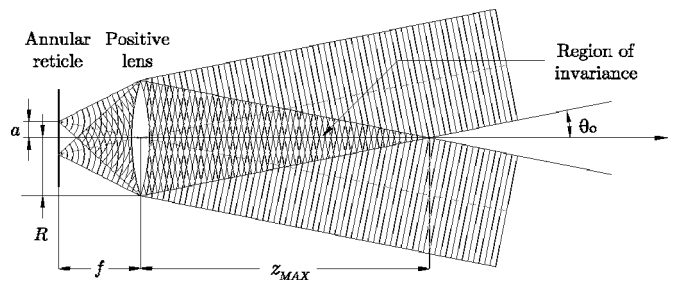


Fig. 9. Schematic representation of the superposition of plane waves after the lens  $L_1$ . Interference will take place at the propagation axis for a distance  $z_{\text{max}}$ .

cannot infer that the phase of the transverse field is shifted by a half wave for each pair of adjacent lobes, which corresponds to the sign reversal of the Bessel functions of the first kind (see Fig. 2).

## B. Angular spectrum of nondiffracting beams

The rings in Fig. 6 correspond to the angular spectrum of the fundamental Bessel beam. Because the only difference in the angular spectra of any two Bessel beams of different order is the angular phase factor  $im\varphi$ , all intensity spectra should look essentially like thin bright rings for any value of  $m$ . Because the ring is formed in the focal plane of  $L_1$ , it will be very intense, and variations along the angular coordinate may be difficult to record in a photograph. It is a good idea to use a neutral density filter before the camera aperture to diminish the intensity of the light and avoid overexposing of the film. A longer focal length of lens  $L_1$  will result in magnification at the Fourier plane, that is, a more extended and hence less intense ring.

Once the experimental setup is assembled, it is straightforward to use different holograms to study the propagation of different classes of fundamental nondiffracting beams. An arbitrary nondiffracting beam can be constructed by complex modulation of its angular spectrum. For instance, we could choose a number of point sources with arbitrary relative phases and amplitudes, and as long as their distance to the optical axis is fixed, a nondiffracting beam of a shape given by the Fourier transform of the point source distribution would result after lens  $L_2$ . It is interesting to verify that due to the Fourier scaling theorem,<sup>25</sup> a smaller hologram will produce a larger ring.

## V. DISCUSSION

We have described a simple experiment to generate computer-generated holograms in the laboratory. Using our experimental technique, an undergraduate physics student can analyze the propagation of several nondiffracting beams. The technique allows for the tailoring of any nondiffracting beam and thus its study in the laboratory. Our experimental technique can be modified to observe an arbitrary field and study its propagation. The holographic technique can be further adapted to reproduce classical experiments<sup>19</sup> with more advanced resources such as greater computational power.

## ACKNOWLEDGMENTS

This work has been supported by the Tecnológico de Monterrey Research Chair in Optics CAT-007, and by

Consejo Nacional de Ciencia y Tecnología México, under Research Grant No. 42808.

- <sup>1</sup>*Laser Devices and Applications*, edited by Ivan P. Kaminow and Anthony E. Siegman (IEEE Press, New York, 1973).
- <sup>2</sup>H. Kogelnik and T. Li, "Laser beams and resonators," *Proc. IEEE* **54**, 97–114 (1966).
- <sup>3</sup>The Amateur Scientist, "Homemade hologram," *Sci. Am.* **216**(2), 122–128 (1967).
- <sup>4</sup>A. G. Porter and S. George, "An elementary introduction to practical holography," *Am. J. Phys.* **43**(11), 954–959 (1975).
- <sup>5</sup>J. S. Marsh and R. C. Smith, "Computer holograms with a desk-top calculator," *Am. J. Phys.* **44**(8), 774–777 (1976).
- <sup>6</sup>X. Chen, J. Huang, and E. Loh, "Computer-assisted teaching of optics," *Am. J. Phys.* **55**(12), 1129–1133 (1987).
- <sup>7</sup>C. W. Leming and O. P. Hastings III, "Computer-generated microwave holograms," *Am. J. Phys.* **48**(11), 938–939 (1976).
- <sup>8</sup>T. Seymour, "Computer simulated holography and computer generated holograms," *Am. J. Phys.* **64**(4), 472–478 (1995).
- <sup>9</sup>J. Turunen, A. Vasara, and A. T. Friberg, "Holographic generation of diffraction-free beams," *Appl. Opt.* **27**, 3959–3962 (1988).
- <sup>10</sup>Z. Bouchal, "Nondiffracting optical beams: Physical properties, experiments, and applications," *Czech. J. Phys.* **53**, 537–578 (2003).
- <sup>11</sup>D. McGloin and K. Dholakia, "Bessel beams: Diffraction in a new light," *Contemp. Phys.* **46**, 15–28 (2005).
- <sup>12</sup>J. J. Miceli, J. Durnin, and J. H. Eberly, "Comparison of Bessel and Gaussian beams," *Opt. Lett.* **13**, 79–80 (1988).
- <sup>13</sup>Z. Bouchal, J. Wagner, and M. Chlup, "Self-reconstruction of a distorted nondiffracting beam," *Opt. Commun.* **151**, 207–211 (1998).
- <sup>14</sup>R. P. MacDonald, S. A. Boothroyd, T. Okamoto, J. Chrostowski, and B. A. Syrett, "Interboard optical data distribution by Bessel beam shadowing," *Opt. Commun.* **122**, 169–177 (1996).
- <sup>15</sup>J. Durnin, J. J. Miceli, and J. H. Eberly, "Diffraction-free beams," *Phys. Rev. Lett.* **58**, 1499–1507 (1987).
- <sup>16</sup>C. A. McQueen, J. Arlt, and K. Dholakia, "An experiment to study a 'nondiffracting' light beam," *Am. J. Phys.* **67**(10), 912–915 (1999).
- <sup>17</sup>J. Durnin, "Exact solutions for nondiffracting beams. I. The scalar theory," *J. Opt. Soc. Am. A* **4**, 651–654 (1987).
- <sup>18</sup>D. N. Moothoo, J. Arlt, R. S. Conroy, F. Akerboom, A. Voit, and K. Dholakia, "Beth's experiment using optical tweezers," *Am. J. Phys.* **69**(3), 271–276 (2001).
- <sup>19</sup>A. W. Lohmann and D. P. Paris, "Binary Fraunhofer holograms, generated by computer," *Appl. Opt.* **6**, 1739–1748 (1967).
- <sup>20</sup>W.-H. Lee, "Sampled Fourier transform hologram generated by computer," *Appl. Opt.* **9**, 639–643 (1970).
- <sup>21</sup>J. Bucklew and N. C. Gallagher Jr., "Comprehensive error models and a comparative study of some detour phase holograms," *Appl. Opt.* **18**, 2861–2869 (1979).
- <sup>22</sup>H. J. Bjelkhagen, *Silver-Halide Recording Materials for Holography and Their Processing*, 2nd ed. (Springer-Verlag, Berlin, 1995).
- <sup>23</sup>J. R. de Bruyn and R. Bradley, "Photographing helium-neon laser light," *Am. J. Phys.* **60**(6), 571 (1992).
- <sup>24</sup>A copy of our Matlab code is available at <http://optica.mty.itesm.mx/pmog/code/>.
- <sup>25</sup>J. W. Goodman, *Introduction To Fourier Optics* (Roberts & Company Publishers, Greenwood Village, 2004).